Airveil: Modulating Finger Friction through Air Cushion Technology for Immersive Surface Haptics

CHEN-KUO SUN, National Taiwan University, Taiwan
CHUN-WEI LIN, National Taiwan University, Taiwan
HSIN-RUEY TSAI, National Chengchi University, Taiwan
BING-YU CHEN, National Taiwan University, Taiwan

Fig. 1. Airveil integrates air-cushion pressure modulation for friction control (left) with real-world shape and material perception in virtual reality (right). By dynamically adjusting the air pressure beneath the fingertip, the device alters frictional resistance and tactile qualities, allowing users to experience variations such as roughness, bumpiness, or adhesiveness while interacting with virtual objects.

We present Airveil, a haptic interface that leverages air cushion effects to dynamically modulate the tangential friction between the fingertip and a surface. By recontextualizing industrial aerostatic lubrication, Airveil regulates airflow through a micro-patterned orifice array to create a pressurized air film. This mechanism enables subtractive friction modulation—physically reducing the coefficient of friction to render a dynamic range of tactile sensations from rough to smooth, while preserving direct finger contact. Airveil's thin and conformal form factor makes it highly adaptable to ungrounded handheld controllers and curved physical 3D props. Technical evaluations characterize the system's wide friction range and geometric adaptability. User studies confirm that Airveil significantly enhances tactile immersion in tangible and mixed-reality scenarios. Results demonstrate that users can reliably distinguish complex material properties and perceive a heightened sense of realism, establishing aerostatic lubrication as a lightweight, high-fidelity approach for enriching materiality in mobile and immersive environments.

Authors' addresses: Chen-Kuo Sun, National Taiwan University, Taipei, Taiwan, chenkuo.sun.tw@gmail.com; Chun-Wei Lin, National Taiwan University, Taipei, Taiwan, blake227@cmlab.csie.ntu.edu.tw; Hsin-Ruey Tsai, National Chengchi University, Taipei, Taiwan, hsnuhrt@gmail.com; Bing-Yu Chen, National Taiwan University, Taipei, Taiwan, robin@ntu.edu.tw.

ACM 2573-0142/2026/8-ARTMHCI8391
https://doi.org/10.1145/3821656

CCS Concepts: • **Hardware** → *Haptic devices*; • **Human-centered computing** → **Haptic devices**; • **General and reference** → **Experimentation**.

Additional Key Words and Phrases: Haptics, Haptic prototype, Air-cushion haptics, Friction modulation, Handheld haptics, 3D model interaction, Material perception, Virtual reality.

ACM Reference Format:
Chen-Kuo Sun, Chun-Wei Lin, Hsin-Ruey Tsai, and Bing-Yu Chen. 2026. Airveil: Modulating Finger Friction through Air Cushion Technology for Immersive Surface Haptics. *Proc. ACM Hum.-Comput. Interact.* 10, 5, Article MHCI8391 (August 2026), 27 pages. https://doi.org/10.1145/3821656

1 INTRODUCTION

Haptic feedback has been widely used to enrich virtual experiences. Friction is a critical and common feedback modality when touching virtual objects and perceiving their roughness. Although previous methods leverage various actuation approaches to modulate friction, authentically rendering multi-level friction force feedback during finger contact and sliding on arbitrary surfaces remains a critical challenge. This gap constrains the sense of realism and materiality in Virtual Reality (VR) and mobile mixed-reality environments. In this work, we aim to bridge this gap by implementing *authentic physical modulation* that alters the actual tribological properties of the interface. Rather than relying on illusions, the system must offer a *wide, tunable friction range*, dynamically reducing resistance from a high-friction baseline (*e.g.*, silicone, $\mu \approx 0.9$) down to effortless sliding ($\mu \approx 0.2$). Crucially, to ensure seamless integration into ungrounded handheld controllers, mobile devices, and complex physical 3D props, this capability must be realized within a *conformal and static form factor*, avoiding the bulk of moving mechanical parts or the material constraints of rigid screens.

Prior research has explored diverse actuation strategies, yet existing technologies struggle to meet all these criteria simultaneously. Mechanical systems utilize moving parts (*e.g.*, wheels or pins) to alter surface geometry [6, 22, 38], but they often suffer from *mechanical latency* and bulkiness. Conventional vibrotactile feedback operates primarily through *perceptual illusion*. By superimposing oscillatory energy, it stimulates mechanoreceptors to create a *phantom sensation* of texture [12, 32], acting as a "mask" rather than modifying the fundamental physical reality of the surface's baseline friction.

Conversely, surface haptic displays can physically alter sliding resistance. Electrostatic methods operate as a fundamentally *additive* mechanism [5, 30]; they can only increase friction above the device's native baseline and remain highly susceptible to environmental humidity and skin impedance. Ultrasonic squeeze-film levitation successfully achieves *subtractive* friction modulation by creating a physical air layer [39]. However, establishing a uniform ultrasonic wave necessitates the use of rigid acoustic resonators (*e.g.*, flat glass or metal plates), severely restricting its conformability and application on ungrounded, curved tangible props.

In this work, we introduce *Airveil*, a novel handheld interface that addresses these challenges by leveraging *air cushion technology* to dynamically vary the tangential resistance between the fingertip and a surface. This mechanism has been widely utilized in industrial non-contact transportation, such as aerodynamic conveyors for product handling [19, 41, 42]. We recontextualize this principle for immersive haptics.

Unlike air-jets that apply kinetic impulses *against* the skin (simulating wind or impact), Airveil generates a pressurized air film between the finger and the surface. This approach fundamentally shifts the interaction paradigm. By lowering the static friction threshold, it physically suppresses the mechanical stick-slip vibrations that cause roughness, allowing users to perceive the surface itself changing—becoming "sticky" or "slippery" on demand—without the intrusion of high-frequency vibrotactile noise or environmental dependencies.

To validate this approach, we developed a compact prototype featuring a micro-patterned orifice array and a silicone contact interface. Guided by the Reynolds equation governing aerostatic lubrication, we optimized key design factors, including orifice density and size, to achieve stable friction modulation in a handheld form factor. Our technical evaluation confirms that Airveil can dynamically tune the static friction coefficient across a wide range. Building on this, we conducted an exploratory user study to characterize how users perceive these aerodynamic changes in terms of roughness, bumpiness, and adhesiveness. Finally, we demonstrate the system's versatility and psychophysical fidelity through a comprehensive VR experience study. We rigorously evaluated Airveil in two scenarios (a VR controller integration and a physical 3D model augmentation) against two distinct baselines: conventional vibrotactile feedback (the industry standard) and physical material props. Our findings reveal that Airveil not only delivers a significantly more immersive and realistic experience than conventional vibration, but also successfully approaches the tactile fidelity of these physical references.

The key contributions of this work are threefold:

(1) *Airveil System & Mechanism:* The design and implementation of a handheld, 3D-model-compatible interface tailored for mobile mixed-reality environments. It leverages *air cushion technology (aerostatic lubrication)* to enable subtractive friction modulation on ungrounded props. This includes a comprehensive design rationale grounded in fluid lubrication theory, detailing the fabrication of the moldable, micro-patterned silicone interface and the characterization of friction behavior under varying pneumatic conditions.
(2) *Perceptual Characterization:* An exploratory study establishing the psychophysical relationship between airflow parameters and tactile perception, identifying *aerostatically modulated friction* as the primary physical driver for simulating diverse material properties (from rubber to ice).
(3) *Empirical Validation:* A rigorous comparative user evaluation demonstrating that Airveil significantly outperforms industry-standard vibrotactile feedback in terms of realism. Crucially, we show that Airveil's tactile fidelity performs closer to *real physical material references*, particularly for rendering low-friction textures on complex physical geometries.

2 RELATED WORK

Our work focuses on an alternative actuation method for friction modulation: the use of air cushion technology. While prior research has applied air cushion effects mainly in the context of non-contact transportation, such as aerodynamic-traction principles for product handling [19], scalable air-levitation conveyors [42], and viscous-traction based contactless conveyors [41], our approach adapts this mechanism for immersive haptics. By recontextualizing air cushions from industrial transport to tactile interfaces, Airveil demonstrates how airflow-based friction modulation can enrich materiality feedback in virtual and augmented reality interactions.

In the following sections, we categorize existing friction feedback interfaces based on their underlying actuation mechanisms: vibration, ultrasound, electrostatics, mechanical systems, material modulation, and finally, air-based feedback.

2.1 Vibration-based Actuation

Vibration is one of the most common approaches for altering perceived friction. Early research on grounded devices demonstrated that varying the amplitude and frequency of mechanically oscillating plates can produce distinct sensations of material roughness [32], or intermittently break finger–surface contact to reduce friction [36].

Beyond stationary setups, vibration has been widely adopted in handheld and wearable devices. Ungrounded haptic styluses [12] reproduce friction cues to enhance pen-based interaction, while

wearable fingertip devices, such as HapCube [18], deliver pseudo-force feedback or directly alter perceived roughness through controlled vibrations on the fingerpad [2]. While these approaches demonstrate that controlled vibration can provide compelling roughness cues, they typically rely on oscillatory signals that simulate texture events rather than modifying the continuous physical friction properties of the surface.

2.2 Ultrasound-based Actuation

Ultrasound-based approaches are foundational to surface haptics, effectively modulating friction through the squeeze-film effect. By inducing high-frequency surface vibrations (typically at resonant frequencies), a physical air layer is trapped and compressed between the fingertip and the plate. This aerostatic pressure lifts the finger, thereby physically reducing the friction coefficient [8, 37]. Foundational devices such as T-PaD [40], STIMTAC [1], and ShiverPaD [11] have successfully utilized this subtractive friction modulation to render textures and distinct tactile edges. Subsequent research has deeply characterized the tribological mechanism of partial squeeze-film levitation [29, 39] and explored its perceptual boundaries [33].

While highly effective, ultrasonic squeeze-film devices fundamentally require the touched surface to act as an actuated resonator. This constraint necessitates the use of rigid, acoustically reflective materials (such as glass or metal) and typically limits implementation to flat screens or grounded trackpads. Extending this uniform ultrasonic resonance to soft, arbitrary, or highly curved 3D physical props in mobile environments remains a significant engineering challenge.

2.3 Electrostatic-based Actuation

In contrast to subtractive ultrasound, electrostatic actuation relies on an additive friction mechanism. By applying a modulating voltage to a conductive layer insulated from the finger, electroadhesion increases the normal force, thereby increasing the tangential friction perceived during sliding [3, 24]. Systems like Teslatouch [5] enable users to feel texture directly on screens. Foundational work has characterized the electrical behavior of these displays [30], while recent advancements have embedded piezoelectric thin films into fully transparent panels [15]. Systems like HaptiDrag [25] have extended electrostatic films over physical objects.

In the domain of portable devices, REVEL [4] introduced "reverse electrovibration," where a signal applied to the body generates an electric field around the fingertips, altering tactile perception when sliding on real surfaces. However, unlike our air cushion approach which enables *subtractive* modulation, electroadhesion is inherently *additive*—it can only increase friction above the baseline. Consequently, it allows for braking effects but physically cannot render the low-friction gliding sensations required for simulating smooth materials.

Similar to ultrasound, electrostatic displays typically require smooth, conductive surfaces and grounded electrical loops, which can restrict their conformability and application on ungrounded, non-conductive tangible props.

2.4 Mechanical-based Actuation

Unlike the high-frequency modulation of vibration or ultrasound, mechanical approaches often involve macroscopic physical changes to the interface. In handheld and wearable contexts, Salazar *et al.* demonstrated that mechanically altering stiffness and friction in VR tangible objects enhances realism [28]. Similarly, HairTouch [20] employs reconfigurable brush hairs, while RollingStone [22] utilizes a slip taxel mechanism for fine texture cues. Expanding on dynamic contact rendering, Haptic Revolver [38] utilizes an actuated wheel that raises and spins beneath the fingertip to render shear forces and motion, utilizing interchangeable wheels to provide varied physical textures. Devices like NormalTouch and TextureTouch [6] provide high-fidelity 3D shape rendering directly on VR

controllers. Additionally, FrictShoes [35] extends mechanical braking to wearable footwear for locomotion. These works highlight the versatility of mechanical actuation in delivering diverse roughness and shape sensations.

However, these systems typically rely on complex moving assemblies (*e.g.*, motors, wheels, or pins) to physically deform the interface, which can introduce bulk and mechanical complexity. In contrast, Airveil achieves friction modulation on a static surface geometry, utilizing airflow to alter tactile properties without the need for macroscopic moving parts at the contact point.

2.5 Material-based and Pneumatic Actuation

Beyond traditional electromechanical mechanisms, researchers have explored material and fluidic approaches to modulate tactile perception. Stick&Slip [23] exemplifies this category by altering fingerpad friction via dynamically applied liquid coatings on arbitrary surfaces. While highly immersive, it relies on consumable fluids and leaves surface residue.

Pneumatic systems offer a clean alternative for delivering versatile tactile feedback. Pneumatic actuators can combine pressure and vibration to enhance stiffness and texture perception [16, 17]. Recently, ViboPneumo [9] demonstrated a finger-worn device that uses pneumatic inflation to physically lift the fingerpad, successfully altering perceived texture roughness in mixed reality without relying on the touched surface's intrinsic material. Furthermore, mid-air systems like Aireal [31] and Ultrahaptics [10] project focused air rings or acoustic waves to create touch sensations via kinetic impulse against the skin, though they inherently lack a physical substrate for the user to rest upon.

2.6 Airveil's Distinctive Features

Collectively, the devices discussed above illustrate diverse strategies for delivering tactile feedback. As highlighted by Wiertlewski et al. [39] and Basdogan et al. [3], creating a physical air film between the finger and the surface is a proven, non-illusory method for subtractive friction modulation.

The primary contribution of Airveil is not the invention of subtractive friction, but rather introducing a novel mechanical pathway to achieve it: *externally pressurized aerostatic lubrication through micro-orifice arrays*. This approach presents profound physical and environmental advantages over both ultrasonic and electrostatic haptic technologies.

Unlike ultrasonic squeeze-film levitation, which strictly requires rigid acoustic resonators (*e.g.*, glass or aluminum) to propagate mechanical waves, Airveil decouples the air supply mechanism from the surface's material resonance. Establishing a uniform ultrasonic squeeze-film necessitates the strict formation of *standing wave resonance*—a condition easily excited on flat, symmetric plates but exceedingly difficult to control on arbitrary, asymmetrical 3D shapes. Furthermore, ultrasonic actuation can inadvertently induce parasitic high-frequency vibrotactile "buzzing" or numbness sensations at certain frequencies. In contrast, Airveil's aerostatic lubrication provides pure physical fluidic support without any high-frequency vibratory interference. This fundamental shift allows our interface to be fabricated from moldable liquid silicone, enabling it to be cast into versatile shapes that effortlessly wrap around ungrounded handheld controllers and arbitrary, curved 3D objects.

Moreover, when compared to electrostatic displays, Airveil operates on a fundamentally different tribological principle. Electroadhesion relies on Coulomb forces to attract the fingerpad, acting as a fundamentally *additive mechanism*—it can only increase tangential resistance. Consequently, electrostatic technology cannot reduce the friction coefficient below the native material's baseline. It is inherently incapable of actively rendering tactile sensations smoother than the physical substrate itself, which fundamentally restricts its dynamic range. Additionally, electrostatic performance is notoriously susceptible to environmental humidity and individual skin impedance (such as finger moisture or dryness). By relying solely on a pneumatic air film, Airveil is completely independent of

the user's skin conductivity and environmental conditions, ensuring absolute stability and consistency in friction modulation.

We acknowledge that pneumatic systems inherently carry trade-offs compared to solid-state ultrasonic or electrostatic screens, including the need for an external compressor (bulkiness) and potential acoustic noise. However, in the context of Virtual and Augmented Reality (VR/AR), these limitations are highly manageable. The spatial audio provided by VR/AR headsets can effectively mask pneumatic operating noise, while tethered setups or wearable haptic backpacks can easily accommodate the required hardware. By accepting these manageable trade-offs, Airveil successfully brings high-fidelity, physical friction modulation out of the flat-screen paradigm and into the realm of tangible mixed reality, where users grasp and interact with irregularly shaped, ungrounded props.

Furthermore, while prior works utilizing air jets or mid-air ultrasound have demonstrated non-contact feedback, they rely primarily on *Kinetic Impulse* (or radiation pressure) to apply a normal force *against* the finger, creating a sensation of impact or "wind-like" flow. In stark contrast, Airveil's *air cushion technology* generates a pressurized air film that modulates the *tangential friction force* between the finger and the surface. This mechanism does not simulate an external force; rather, it modifies the perceptible *surface properties*, allowing for the rendering of varying textures without the intrusion of air turbulence. This distinction clarifies why our approach offers a tactile experience that is qualitatively different from the impact-based sensations commonly found in air-jet displays.

3 AIRVEIL DESIGN AND IMPLEMENTATION

We designed a prototype system, Airveil, to explore the potential of leveraging the air-cushion effect for modulating frictional forces between the fingertip and a surface. This section details the design rationale, hardware configuration, and hardware measurements of the system.

3.1 Design Considerations

Theoretical Basis. The fundamental principle of Airveil is *aerostatic lubrication*, where a pressurized air film separates the fingertip from the substrate. To achieve controllable friction modulation, the system must generate sufficient lift force to counteract the user's normal finger pressure. The stability and tactile quality of this air film are not determined by a single factor, but by the complex interplay between *supply pressure*, *surface geometry*, and *finger dynamics*.

To model these interactions and optimize our design, we refer to the Reynolds equation for compressible fluid lubrication [27]:

$$\frac{\partial}{\partial x}\left(ph^3\frac{\partial p}{\partial x}\right) + \frac{\partial}{\partial y}\left(ph^3\frac{\partial p}{\partial y}\right) = 6\eta U\frac{\partial ph}{\partial x} \tag{1}$$

where p is the air pressure distribution, h is the air film thickness (clearance), η is the air viscosity, and U is the sliding velocity of the finger. The left-hand side of the equation represents the *pressure-driven flow* generated by our pneumatic system (the air cushion effect), while the right-hand side accounts for the *shear-driven flow* induced by the user's finger movement (the aerodynamic wedge effect).

This mathematical relationship highlights that the tactile sensation is directly governed by the spatial uniformity of the pressure distribution px, y. A continuous and uniform pressure field results in a stable lift force (perceived as smoothness), whereas significant pressure gradients created by sparse orifice spacing result in periodic force fluctuations (perceived as bumpiness). This theoretical framework guided our selection of the following key design parameters:

Effective Area. We selected an effective area of 1.5 $\times$ 1.5 cm to provide sufficient space for fingertip movement while maintaining consistent air-cushion coverage. This range was also chosen

to balance portability for potential handheld use, as larger areas would require greater airflow that exceeds the limitations of the input tubing diameter.

Air Orifice Density. The density of air orifices dictates the continuity of the supporting air film (the px, y uniformity). In our design, orifices are distributed within the 1.5 × 1.5 cm area in three configurations: 6×6 (3.0 mm pitch), 5×5 (3.75 mm pitch), and 4×4 (5.0 mm pitch). According to the lubrication model, the 6×6 array (high density) minimizes the pressure drop between adjacent orifices, approximating a continuous pressure profile that users perceive as a smooth, low-friction surface. In contrast, the 4×4 array (low density) introduces significant spatial pressure gradients ("pressure dips") between orifices. As the finger traverses these gradients, the periodic fluctuation in lift force is mechanically decoded by the skin as surface unevenness or "bumpiness." Thus, varying the orifice density serves as a key design parameter, allowing us to modulate tactile perception between a textured, bumpy surface (sparse array) and a seamless, lubricated state (dense array).

Air Orifice Size. Preliminary observations indicated that overly large orifices caused airflow to diffuse like a turbulent jet, while overly small ones produced sharp, uncomfortable pressure points. Viewing the orifice as a flow restrictor in the theoretical model, we selected sizes (0.08 mm and 0.1 mm) that ensure the primary pressure drop occurs at the bearing gap (h) rather than the supply line. This maximizes the stiffness of the air cushion, forming a uniform film without excessive dispersion or localized jets.

Air Pressure. The magnitude of the input air pressure (p) directly governs the degree of normal force reduction. Higher pressure produces stronger cushioning and more noticeable friction reduction (subtractive modulation). Conversely, lower pressure results in a sensation of rougher, stickier friction. In sparser configurations (*e.g.*, 4×4), lower pressure can further accentuate the "grainy" texture due to insufficient lift in the gaps between orifices.

Surface Material. We selected liquid silicone rubber (LSR) with a hardness of 20A. This choice was motivated by its high baseline friction and adhesion, which enhances the perceptual contrast (dynamic range) when friction is reduced by the air cushion. Additionally, LSR's molding properties allowed us to cast a thin layer (approx. 2–3 mm) directly onto the prototype, balancing comfort with tactile sensitivity. The silicone layer was patterned with openings aligned to the orifice arrays to prevent obstruction of the airflow.

Air Chamber Design. While the chamber size does not directly determine the air cushion's formation (which is governed by orifice geometry), it impacts pneumatic response. We designed a compact chamber to prioritize portability and minimize the volume of compressible air, thereby reducing response delay. The chamber features a replaceable top cover, enabling rapid swapping between different orifice patterns for flexible experimentation.

3.2 Device Implementation

Based on the design considerations, we implemented a prototype composed of three main components: the air chamber, the interchangeable surface plates, and the silicone top layer. Both the air chamber and the surface plates were 3D printed. A thin layer (2–3 mm) of liquid silicone rubber (20A hardness) was cast over the surface plate. To create the orifice openings, metal wires corresponding to the intended orifice diameter were inserted into the silicone layer while it was still uncured. After the silicone cured, the wires were carefully removed, leaving precise openings for airflow (see Figure 2).

The resulting surface provided a durable tactile interface while preserving the airflow path. The replaceable surface plates allowed us to easily switch between different orifice densities (4×4, 5×5, 6×6) and sizes (0.08 mm, 0.1 mm), enabling systematic evaluation of friction modulation under various conditions.

The Airveil prototype, illustrated in Figure 3a, features a handheld cylindrical air chamber connected via a 0.8 cm diameter pneumatic tube to an SMC ITV2050 Electro-Pneumatic Regulator. The

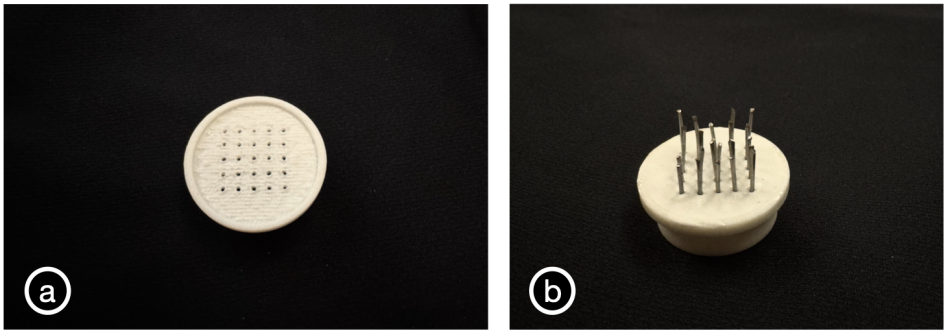

Fig. 2. Prototype fabrication process: (a) 3D-printed air chamber cover; (b) liquid silicone rubber layer with inserted metal wires to form orifice openings.

valve is further connected to an air compressor cylinder, providing regulated airflow to the chamber. Control of the system is achieved using an MSI Vector series laptop interfaced with an ESP32 microcontroller, which adjusts the valve output in real time to modulate air pressure and fingertip friction. To characterize the system's temporal response, we measured the end-to-end actuation latency from the initiation of a software command to the physical force modulation detected by an IMADA digital force gauge. Across our tested operational pressure range (0.05 to 0.23 bar), the average latency over 10 repeated trials per pressure level consistently remained between 25 and 30 ms. This rapid response time falls well within the acceptable threshold for human tactile perception, ensuring a highly responsive and synchronized real-time haptic experience.

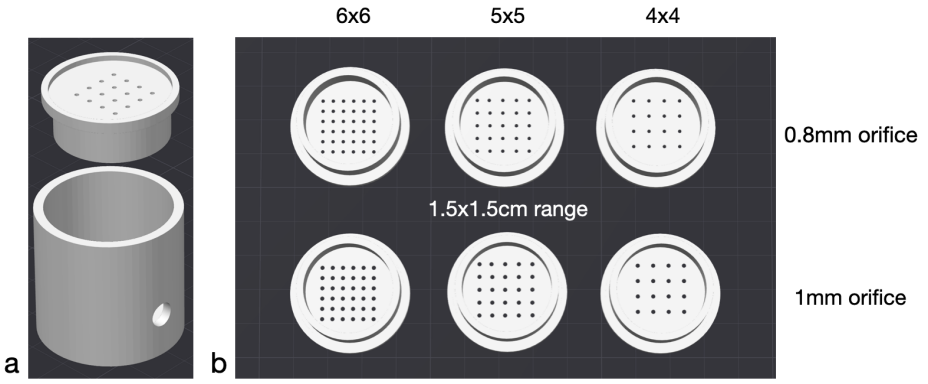

Fig. 3. Airveil prototype (a) with air chamber, cover, and tubing connector; (b) interchangeable surface plates with different orifice densities (4×4, 5×5, 6×6) and diameters (0.08 mm, 0.1 mm).

3.3 Technical Evaluation

To evaluate the effectiveness of our prototype, we tested six surface configurations (Figure 3b) that combined three levels of orifice density (4×4, 5×5, and 6×6 arrays) with two orifice sizes (0.08 mm and 0.1 mm). For each configuration, we specifically quantified the static friction force under varying levels of applied air pressure to examine how orifice parameters influence frictional behavior.

Our evaluation deliberately focuses on static friction rather than dynamic friction due to the inherent tribological complexities of human skin and the localized spatial constraints of our micro-orifice array. When a fingertip begins to slide across a surface, it initially undergoes a "pre-slip" phase. During this phase, the viscoelastic skin shears and deforms laterally for approximately 3 to 8 mm before breaking contact to initiate true macroscopic sliding [13, 21]. Because our active orifice array spans a highly localized area of only 1.5 cm (15 mm), the finger spends a substantial fraction of the interaction period within this static, pre-slip deformation state. In such micro-patterned regions, capturing stable dynamic friction is highly susceptible to biological artifacts and continuous skin deformation. Consequently, the peak static friction serves as the most reliable and physically representative metric for localized contact resistance [34].

Furthermore, from a psychophysical perspective, static friction is the fundamental determinant of the overall tactile sensation, encompassing both macroscopic resistance and microscopic texture. While bulk static friction directly dictates the perceived adhesiveness or stickiness of a surface, the sensation of roughness is largely driven by high-frequency vibrotactile cues generated by the stick-slip phenomenon during active exploration [7, 14]. The severity and amplitude of these stick-slip vibrations are directly governed by the upper threshold of static friction. As demonstrated in prior surface haptic studies, partially levitating the fingerpad physically reduces the real solid-to-solid contact area [39]. By utilizing an air cushion to significantly lower the static friction threshold, Airveil inherently mitigates both the macroscopic dragging resistance and the mechanical stick-slip mechanism. Consequently, measuring the reduction in static friction provides valid, quantifiable physical evidence of the system's capacity to modulate overall surface adhesiveness and attenuate the vibrotactile noise underlying tactile roughness.

3.3.1 Evaluation Design. To evaluate the static friction behavior, we tested the six surface configurations described above. For each configuration, measurements started at 0 bar and increased in 0.02 bar increments from 0.05 bar, which is the minimum achievable pressure of our control valve, up to 0.23 bar, resulting in a total of 11 pressure levels per configuration.

During testing, a 200 g weight was placed on a square base roughly the size of a fingertip, with a contact area of 1 × 1 cm. The base was 3D printed and connected via a string to an IMADA force gauge, which recorded forces in Newtons (N). A stepper motor was used to gradually apply force until the base began to move, and the maximum instantaneous force at the onset of movement was taken as the sliding onset force. To ensure measurement consistency, the setup was mounted on an aluminum extrusion frame, which served as a fixed platform to guarantee that the pulling force applied by the motor remained parallel to the weight.(Figure 4a)

Due to the air-cushion effect, an upward force partially counteracts the normal force applied by the weight. Therefore, for each configuration and pressure level, we first measured the upward air force. The effective normal force N was then calculated as the weight minus the measured upward force. The static friction coefficient μ was computed using the classical relation $F = \mu N$, where F is the measured sliding onset force.(Figure 4b)

3.3.2 Evaluation Results. Figure 5 illustrates the general relationship between input air pressure and the measured static friction coefficient (μ) across all orifice configurations. At baseline (0 bar), all configurations exhibited a consistent static friction coefficient of approximately $\mu \approx 0.95$, confirming

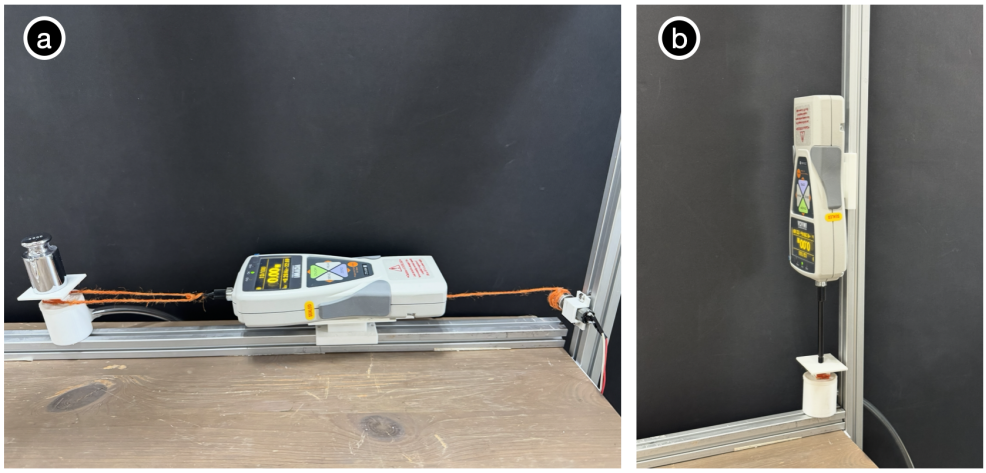

Fig. 4. Experimental setup for static friction measurement (a), consisting of a 200 g weight, IMADA force gauge, and stepper-motor pulling system mounted on an aluminum extrusion frame to ensure parallel force application; (b) Calculation process of the effective normal force and static friction coefficient, accounting for the upward air force generated by the air-cushion effect.

Air pressure / Pattern	0bar	0.05bar	0.07bar	0.09bar	0.11bar	0.13bar	0.15bar	0.17bar	0.19bar	0.21bar	0.23bar
6x6 0.08cm	0.955	0.721	0.622	0.552	0.478	0.419	0.361	0.316	0.322	0.294	0.384
5x5 0.08cm	0.935	0.696	0.701	0.718	0.63	0.568	0.503	0.481	0.36	0.317	0.311
4x4 0.08cm	0.89	0.747	0.717	0.717	0.594	0.589	0.515	0.459	0.452	0.326	0.387
6x6 0.1cm	0.894	0.682	0.563	0.545	0.463	0.397	0.304	0.227	0.233	0.248	0.276
5x5 0.1cm	0.918	0.724	0.627	0.568	0.502	0.439	0.435	0.437	0.324	0.267	0.28
4x4 0.1cm	0.934	0.76	0.737	0.632	0.558	0.5	0.489	0.489	0.366	0.351	0.275

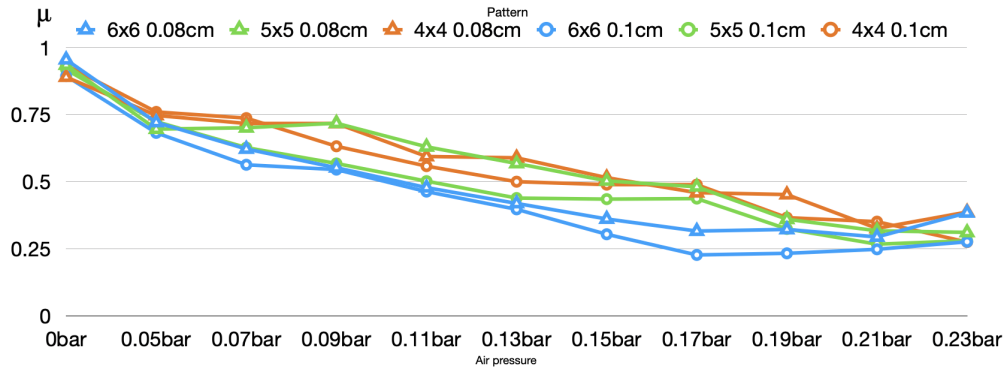

Fig. 5. Evaluation results of static friction coefficients across different orifice densities and sizes under varying air pressures.

a uniform initial surface property dominated by the silicone material. As air pressure increased, we

observed a significant monotonic decrease in the friction coefficient across all configurations. On average, an increment of 0.04 bar resulted in a reduction of approximately 0.2 in μ, with high air pressures reducing the coefficient to around 0.3.

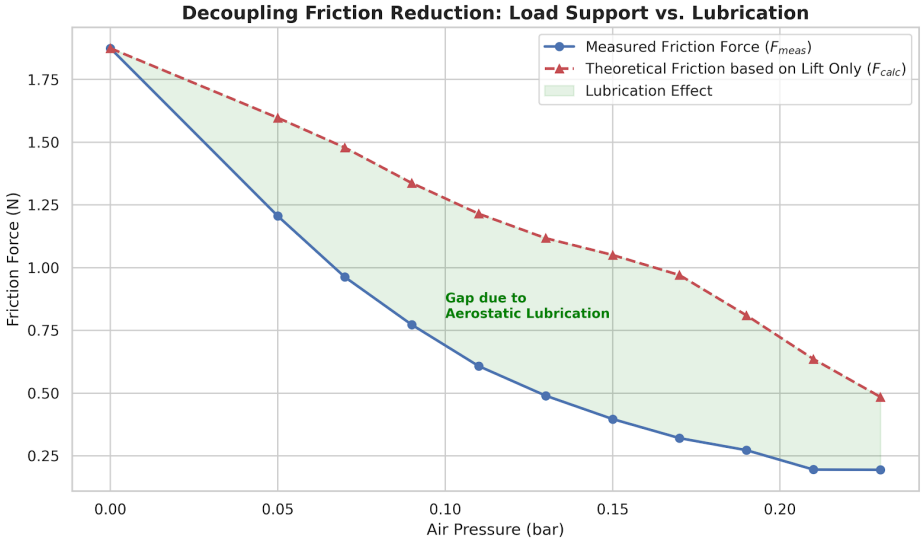

Fig. 6. Analysis of friction reduction mechanisms (Data from 6×6, 0.08 mm configuration). The *red dashed line* represents the theoretical friction force if the reduction were driven solely by the decrease in net normal force (assuming a constant $\mu \approx 0.955$). The *blue solid line* shows the actual measured friction force. The significant divergence between the two curves highlights the contribution of aerostatic lubrication, which alters the interfacial properties and reduces shear resistance beyond simple load bearing.

Mechanism Validation: Lubrication vs. Normal Force. To investigate the underlying mechanism, we isolated the data for the 6×6 (0.08 mm) configuration and compared the measured friction force against a theoretical model based solely on normal force reduction (Figure 6). If the friction reduction were caused only by the pneumatic lift countering the finger's load (Coulomb friction model: $F = \mu_{const} \times W - F_{lift}$), the friction force would follow the *red dashed line*. However, our measurements (*blue solid line*) show a much steeper decline. For instance, at 0.17 bar, while the net normal force was reduced by approximately 48%, the actual friction force dropped by nearly 83%. This discrepancy confirms that Airveil operates primarily through *aerostatic lubrication*: the formation of a pressurized air film separates the finger from surface asperities, drastically lowering the effective friction coefficient (μ) itself, rather than just the normal load.

Operational Limits and Instability. At the highest tested pressure of 0.23 bar, some measurements (*e.g.*, for the 6×6 configuration) showed an increase rather than a decrease in friction. This is likely due to *pneumatic instability* caused by excessive airflow turbulence, which disrupts the stable air film. However, this instability was not universal. *For the 4×4 configuration with 0.1 mm orifices, the friction coefficient decreased steadily and reliably even at 0.23 bar.* All measured data are reported for completeness; but based on this observation, in subsequent experiments, only the 4×4 configuration (0.1 mm) utilized the 0.23 bar pressure setting, justifying its inclusion where stable modulation was maintained.

In summary, these results demonstrate that Airveil effectively modulates friction through two coupled mechanisms: global pressure control (driving the transition to lubrication) and orifice pattern design (tuning the film uniformity). By managing these parameters, the system achieves a wide dynamic range of tactile properties.

4 EXPLORATORY STUDY

In this exploratory study, we aimed to investigate whether participants could distinguish and subjectively evaluate variations in friction generated by our system.

We designed a friction mapping task in which participants interacted with different surface conditions created by Airveil. The focus was on non-visual exploration, where participants relied solely on touch to assess differences in roughness, bumpiness, and adhesiveness. By analyzing their subjective ratings, we aimed to understand the discriminability of our friction modulation system. Additionally, participants were asked to associate the perceived sensations with familiar material qualities to capture their intuitive interpretations of the tactile experiences.

4.1 Design and Procedure

At the beginning of the experiment, participants were introduced to the overall procedure and given the opportunity to briefly explore the hardware prototype. We explained the three frictional dimensions to be evaluated in this study, Roughness, Bumpiness, and Adhesiveness, which were selected based on prior psychophysical findings on tactile texture perception [5, 26], and tailored to the capabilities of our device.

Participants then followed our instructions to wear noise-canceling headphones playing white noise, ensuring that auditory cues did not interfere with their tactile perception. Using their index finger, they explored the surface of our device. To ensure experimental consistency, participants were guided to maintain a normal force of approximately 0.4–0.6 N throughout the tasks. A force sensor placed beneath the device was used to monitor the applied normal force in real-time. This range was selected to replicate the typical contact force applied during natural texture exploration, minimizing the potential confounding effects of pressure variations. Within this constraint, participants were encouraged to interact with the surface in a natural manner to elicit authentic tactile impressions.

Roughness: the perceived smoothness or graininess of the surface, ranging from extremely smooth (*e.g.*, glass) to highly coarse (*e.g.*, sandpaper). A higher rating indicated a perception of greater coarseness.

Bumpiness: the perceived sense of unevenness or three-dimensional texture, ranging from completely flat to distinctly raised or indented. A higher rating indicated a stronger perception of unevenness or protrusion.

Adhesiveness: the perceived resistance between the finger and the surface, akin to a sticky or suction-like sensation, ranging from very slippery to highly adhesive. A higher rating indicated a stronger perception of stickiness or suction-like resistance.

Participants rated each dimension using a 7-point Likert scale during non-visual exploration (touch only).

To prevent order effects, the 14 friction conditions (12 air-cushion–modulated conditions across 4 orifice patterns, 1 baseline with 0 bar, and 1 smooth reference condition at 0.2 bar) were presented in a fully randomized sequence for each participant. For the 12 modulated conditions, we selected air pressures based on corresponding friction coefficients across the four orifice patterns, so that the comparisons were grounded in frictional equivalence rather than raw pressure values (Figure 7). Since the tactile impressions of the 5×5 and 6×6 orifice patterns were found to be highly similar, we focused our user testing on the 6×6 and 4×4 patterns to better capture perceptual distinctions.

	0bar	0.05bar	0.07bar	0.09bar	0.11bar	0.13bar	0.15bar	0.17bar	0.19bar	0.21bar	0.23bar
6x6 0.08cm	0.955	0.721	0.622	0.552	0.478	0.419	0.361	0.316	0.322	0.294	0.384
5x5 0.08cm	0.935	0.696	0.701	0.718	0.63	0.568	0.503	0.481	0.36	0.317	0.311
4x4 0.08cm	0.89	0.747	0.717	0.717	0.594	0.589	0.515	0.459	0.452	0.326	0.387
6x6 0.1cm	0.894	0.682	0.563	0.545	0.463	0.397	0.304	0.227	0.233	0.248	0.276
5x5 0.1cm	0.918	0.724	0.627	0.568	0.502	0.439	0.435	0.437	0.324	0.267	0.28
4x4 0.1cm	0.934	0.76	0.737	0.632	0.558	0.5	0.489	0.489	0.366	0.351	0.275

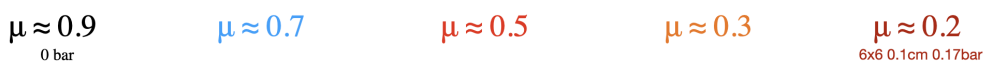

Fig. 7. Selection of friction conditions for user testing, showing how equivalent friction coefficients were used to compare 4×4 and 6×6 orifice patterns.

After completing the ratings for Roughness, Bumpiness, and Adhesiveness, participants were asked to associate the perceived sensations with familiar material qualities. The provided material set included: wood, textiles (cotton, denim), burlap, glass, stone, oil, velvet, metal, rubber, plastic, and sandpaper. Participants could also annotate specific surface impressions (*e.g.*, "wood with grain").

Finally, participants provided two additional subjective ratings (7-point Likert scale):

Satisfaction rating: indicating how reasonable and convincing participants found the friction parameters in reflecting the intended tactile qualities. A higher rating indicated that the parameters were more consistent with their subjective evaluations of roughness, bumpiness, and adhesiveness.

Interference rating: Interference rating: indicating whether and to what extent the air-cushion effect itself interfered with their perception of the material's frictional qualities. A higher rating indicated lower perceived interference from the air-cushion effect.

After experiencing all 14 conditions, participants were allowed to revisit and adjust their ratings during a refinement phase.

4.2 Participants

Twelve participants (aged between 23 and 34, six women and six men) took part in this study. All participants were right-handed, and their fingers were cleaned prior to touching the device to minimize residue effects. During the experiment, none of the participants reported any discomfort.

4.3 Results

Figure 8 presents the relationship between the static friction coefficient (μ) and user-perceived roughness, analyzed via a unified Linear Mixed-Effects Model (LMM). To robustly account for individual baseline rating variances, participant ID was modeled as a random effect, while Friction, Orifice Pattern (4×4 vs. 6×6), and Hole Size (0.08 mm vs. 0.1 mm) were incorporated as fixed effects. The figure displays the raw data distribution (scatter points) alongside the fixed-effect trend lines and their 95% confidence intervals (shaded regions).

The multivariate LMM revealed two highly significant independent predictors for perceived roughness. First, the absolute physical friction demonstrated a dominant main effect ($p = 0.003$), confirming that the reduction of static friction via the aerostatic film fundamentally dictates a smoother tactile sensation. Second, the model identified Hole Size as a critical independent factor ($p = 0.001$). As visualized in Figure 8, This indicates that the geometric contribution to perceived roughness is not absolute, but strictly density-dependent. For the dense 6x6 array, increasing the orifice size from 0.08 cm to 0.1 cm exacerbated the surface discontinuity, leading to a notable increase

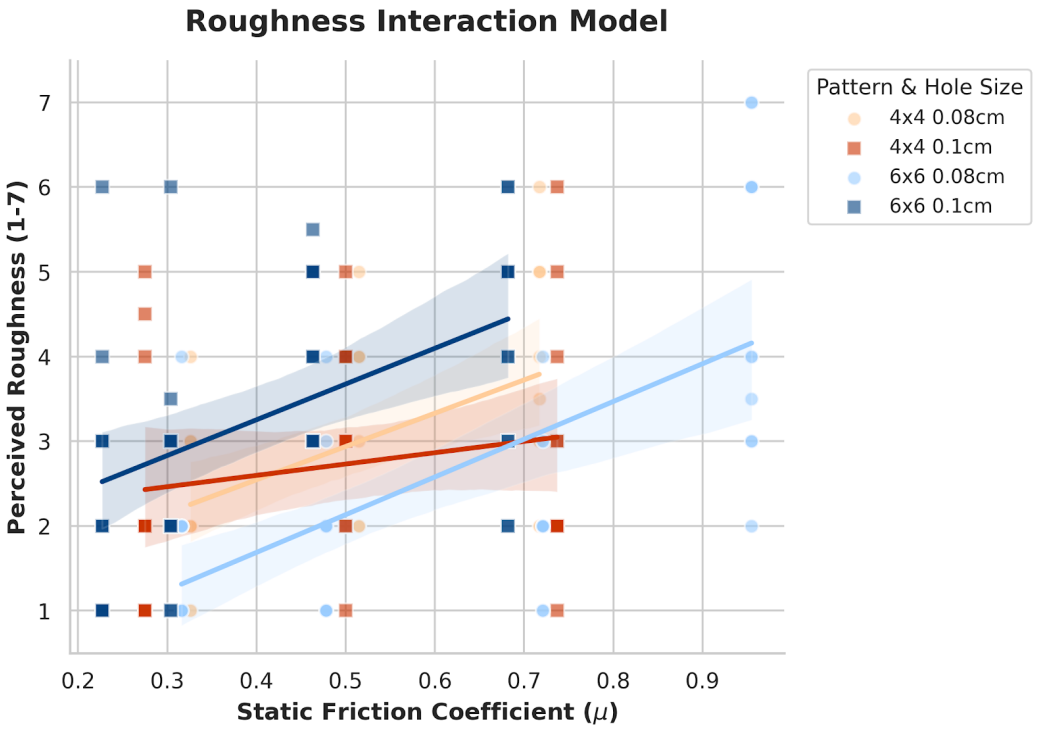

Fig. 8. Linear Mixed Model (LMM) regression showing the relationship between static friction coefficients and participants' perceived roughness ratings. The trend line represents the fixed effect, accounting for individual participant variability.

in perceived roughness. Conversely, for the sparse 4x4 array, enlarging the orifices to 0.1 cm did not increase roughness; rather, it resulted in a slight reduction (mean rating decreased from 3.01 to 2.73). This suggests that in sparse configurations, the increased localized airflow from larger orifices may provide marginally better lift, counteracting the geometric edges.

Interestingly, the interaction between Friction and Orifice Pattern was not statistically significant ($p = 0.305$) in this comprehensive model. This suggests that the fundamental perceptual mapping—where less friction equals less roughness—holds universally true across our tested micro-pattern configurations.

To rigorously evaluate how hardware parameters and air pressure influence perceived bumpiness, we employed a Linear Mixed-Effects Model (LMM). Participant ID was modeled as a random effect, while Air Pressure, Orifice Pattern (4×4 vs. 6×6), and Hole Size (0.08 mm vs. 0.1 mm) were incorporated as fixed effects. To capture the nuanced structural effects, we specifically included the interaction term between Orifice Pattern and Hole Size.(Figure 9)

The multivariate analysis revealed a highly significant interaction effect between Orifice Pattern and Hole Size ($p < 0.001$). This indicates that the impact of orifice diameter on perceived bumpiness fundamentally depends on the spatial density of the array. Specifically, for the dense 6×6 configuration, enlarging the orifices from 0.08 mm to 0.1 mm drastically increased the perceived bumpiness (mean rating shifted from 2.50 to 4.09). Conversely, for the sparse 4×4 configuration, increasing

the orifice size did not enhance bumpiness; in fact, the ratings remained consistently high and even exhibited a slight decrease (mean rating 4.40 vs. 4.16).

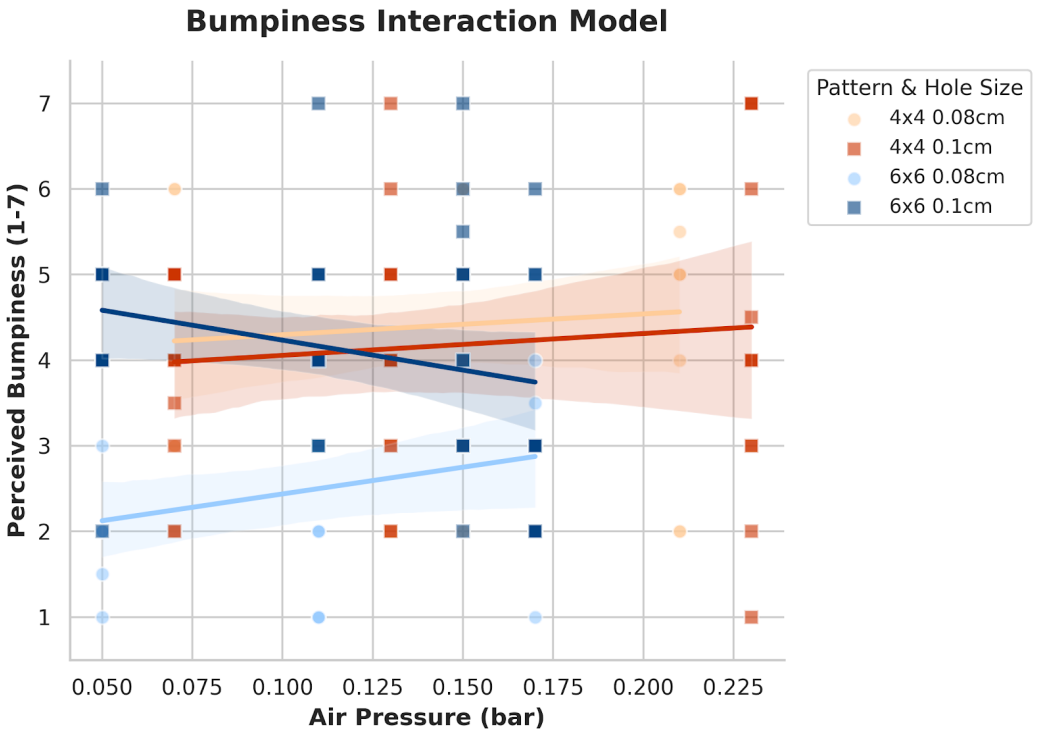

Fig. 9. Linear Mixed Model (LMM) regression illustrating the correlation between applied air pressure and perceived bumpiness ratings. The model accounts for individual baseline differences across participants.

Furthermore, Air Pressure ($p = 0.323$) did not demonstrate a significant main effect on bumpiness. This suggests a critical decoupling in our parameter design: while modulating global air pressure effectively alters macroscopic friction and roughness, it does not significantly mask the spatial perception of structural bumpiness. Instead, perceived bumpiness is predominantly governed by the geometric interplay between orifice size and spatial density. To minimize bumpiness and achieve a "smoothness baseline," a dense array with small orifices (*i.e.*, , 6×6 0.08 mm) is strictly required. In comparison, at lower pressures, users perceived bumpiness in the 6×6 0.1 mm configuration comparable to the sparse 4×4 patterns, attributed to the larger orifice diameter.

To robustly analyze the perceived adhesiveness, we maintained our unified statistical approach, employing a Linear Mixed-Effects Model (LMM). As with previous dimensions, participant ID was modeled as a random effect, while Friction, Orifice Pattern, and Hole Size, along with the interaction between Pattern and Hole Size, were incorporated as fixed effects.

The multivariate analysis revealed a highly significant and overwhelmingly dominant main effect for the static friction coefficient ($p < 0.001$). This confirms that surfaces engineered to exert higher bulk static friction were consistently judged as more adhesive. As visualized in Figure 10, the data points for all hardware configurations follow a tight upward trajectory, establishing macroscopic static friction as a highly reliable and universal predictor of perceived stickiness.

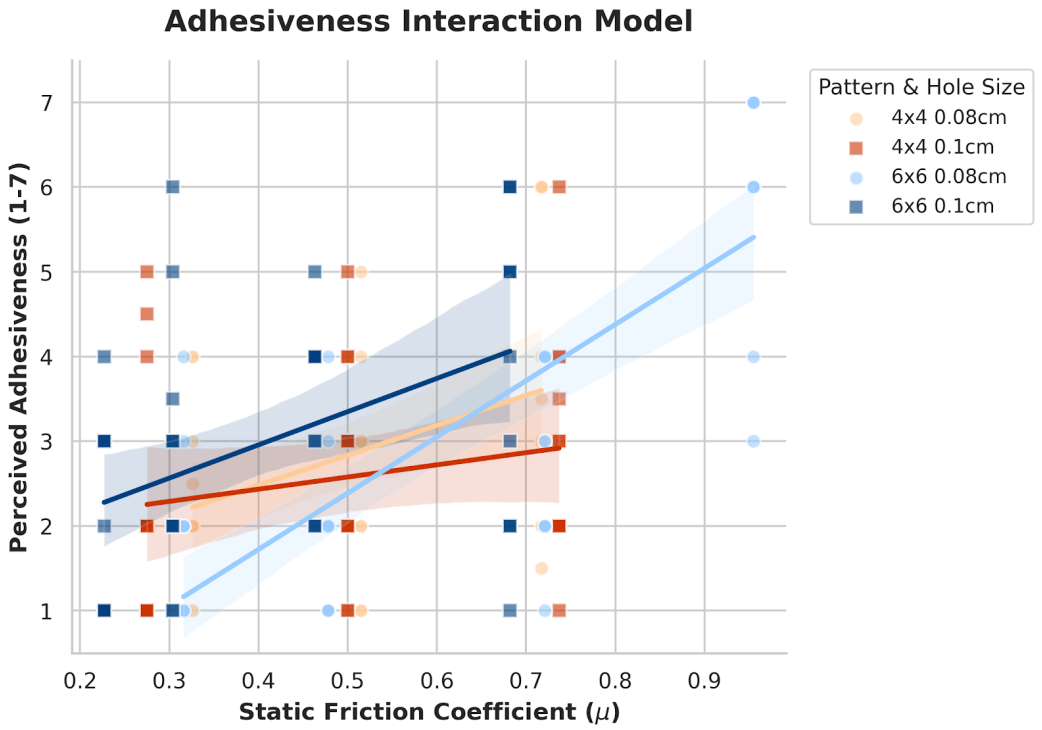

Fig. 10. Linear Mixed Model (LMM) regression demonstrating the relationship between static friction coefficients and participants' perceived adhesiveness ratings. The trend line represents the fixed effect, accounting for individual participant variability.

In contrast, the geometric configuration of the orifice patterns played a minimal role in adhesiveness perception. The main effects for both Orifice Pattern ($p = 0.488$) and Hole Size ($p = 0.371$) were not statistically significant. While a minor interaction effect between Pattern and Hole Size was detected ($p = 0.007$), the absolute variance in mean adhesiveness ratings introduced by structural geometry was negligible compared to the variance driven by friction. This indicates that while geometric features drastically alter the spatial texture (roughness and bumpiness), they do not independently drive users' bulk stickiness judgments.

Notably, the statistical dominance of friction in predicting adhesiveness ($z = 9.80$, $p < 0.001$) is markedly stronger than its effect on roughness ($z = 3.86$, $p < 0.001$). This distinction suggests a fundamental perceptual dichotomy in subtractive haptics: Airveil's air-cushion mechanism excels at modulating bulk retarding forces (perceived as macroscopic stickiness or braking). In contrast, the perception of roughness relies on the intermittent stick-slip phenomena induced by the air bearing, which provides a perceptible structural coarseness, yet is more susceptible to modulation by local geometric interactions.

In terms of consistency (inter-participant agreement), users demonstrated some convergence in their material associations under specific conditions. Notably, when static friction was very high, participants consistently associated the sensation with rubber—as one participant described, "It really feels sticky, like my finger is dragging on rubber." However, in most other cases, the associations were considerably diverse, reflecting the inherently subjective nature of tactile description. For example,

some users(P2, 7, 9, 12) described the same mid-level condition as “like polished wood”, while others noted “it reminds me of leather, smooth but with some grip.”

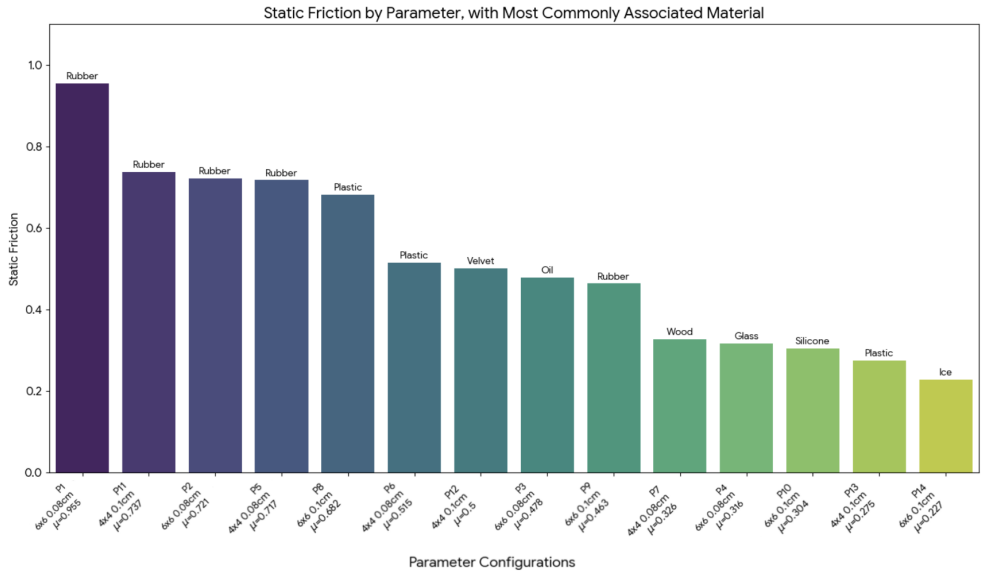

Fig. 11. Distribution of material associations across friction levels.

Statistical analysis further revealed a significant relationship between material associations and static friction. The overall trend followed the order: rubber > plastic > wood > glass > ice, which closely mirrors the descending scale of static friction values. Among the vocabulary used, the most frequent descriptors were rubber, wood, ice, plastic, and leather, representing the core material terms participants relied on to express varying frictional sensations. (Figure 11)

Beyond material associations, we analyzed the relationship between perceived interference and user satisfaction. Our analysis revealed a moderate *negative* correlation (r = -0.37) between the two variables. Generally, minimizing pneumatic disturbance leads to higher satisfaction; indeed, the baseline condition (P1), which had the lowest interference rating (Mean = 1.82), achieved the highest satisfaction score (Mean = 5.86). This result is directly attributable to the fact that P1 operates at zero air pressure, thereby completely eliminating any sensation of escaping air.

However, a closer examination reveals an interesting trade-off at high-pressure levels. While stronger airflow (*e.g.*, P4, P10, P13, P14, $\mu \approx 0.2$) significantly increased perceived interference (Mean $\approx$ 5.0) due to the sensation of escaping air, satisfaction ratings remained surprisingly resilient (Mean $\approx$ 5.3). This suggests that while users found the high-velocity airflow physically distracting, they appreciated the functional benefit of the "super-smooth" gliding sensation enough to tolerate the disturbance. (Figure 12)

Participant interviews provided context for these quantitative trends. Under high-pressure conditions, users often reported that the sensation of air escaping became a primary focus, contributing to the higher interference scores. Participants (P3, P4, P6) noted, “When the pressure is too strong, it feels distracting—I pay more attention to the air than to the material itself.” Conversely, low-pressure conditions were associated with stronger contact and adhesion, described by users as “more directly

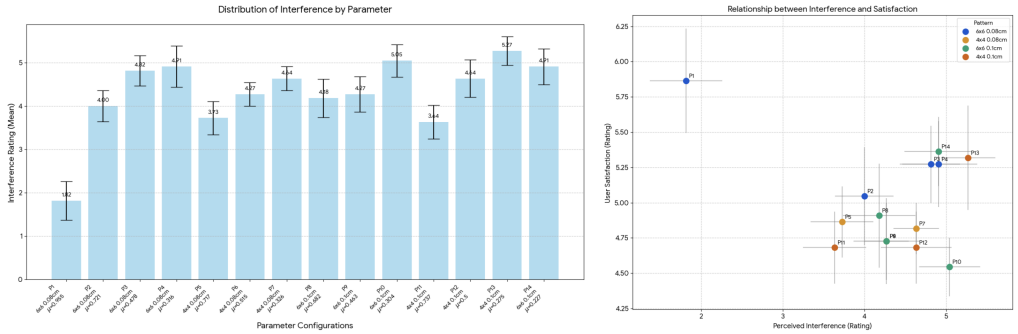

Fig. 12. Correlation analysis of interference and satisfaction.

connected to the object, almost like the silicone material itself." Ultimately, while moderate pressure levels provided the most convincing balance for general material impressions (P4: "When the bumpiness isn't too strong, it's easier to imagine materials"), the data indicates that users are willing to accept a certain degree of pneumatic interference to experience the unique, low-friction capabilities of the system.

5 USER STUDIES

To examine how the tactile feedback generated by Airveil influences users' VR experiences, we designed two demonstration scenarios and conducted a VR experience study. Crucially, to address the psychophysical fidelity of our system, we evaluated Airveil against two distinct baselines: conventional vibrotactile feedback (the industry standard) and physical material props.

In the first scenario, participants used a VR controller equipped with Airveil to explore six different virtual material textures through direct fingertip contact (Figure 13a). In the second scenario, Airveil was integrated into physical 3D models that were mapped onto their virtual counterparts, allowing users to simultaneously perceive both object shape and customizable surface textures in VR (Figure 13b).

We formulated the following hypotheses based on the physical mechanisms involved:

- H1 (Realism): Airveil will yield significantly higher realism ratings than conventional vibration, performing closer to the real physical material references. This effect will be particularly pronounced for low-friction materials (*e.g.*, Ice, Glass), as Airveil physically reduces surface resistance rather than adding oscillatory noise.
- H2 (Integration): Integrating Airveil into physical 3D objects will maintain high tactile fidelity, demonstrating the method's adaptability to complex geometries beyond flat surfaces.

5.1 Design and Procedure

At the beginning of the study, participants were introduced to the overall procedure and briefed on the Airveil technology. To rigorously evaluate the system's versatility across distinct application domains while controlling for individual tactile sensitivity, we employed a strictly within-subjects (repeated-measures) design. All participants experienced both demonstration scenarios (VR Controller Integration and Physical Prototyping Integration) and evaluated the target materials across all three feedback conditions (Airveil, Vibrotactile, and Physical Material Props).

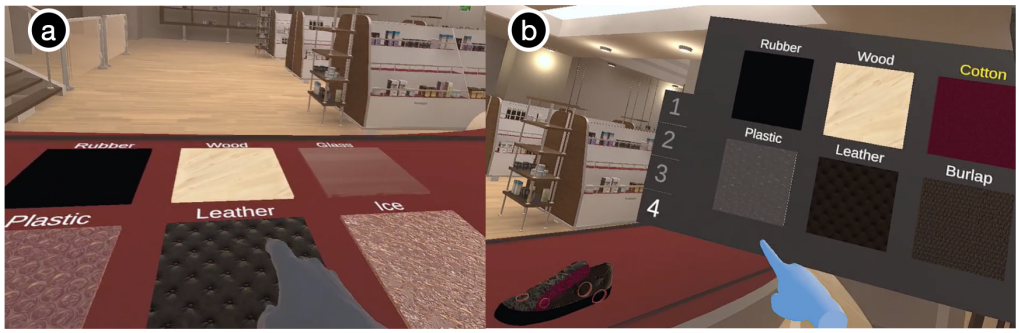

Fig. 13. Demonstration scenarios for the VR experience study. (a) Airveil mounted on a VR controller, allowing participants to explore six virtual material textures via direct fingertip contact; (b) Airveil integrated into physical 3D models, enabling simultaneous perception of object shape and customizable surface textures in VR.

Fig. 14. Airveil demonstration setups. (a) Airveil mounted on a VR controller using a support frame; (b) Physical 3D models (a shoe and a humanoid figure) integrated with Airveil; (c) The reference set of physical material props used to establish ground-truth tactile expectations.

5.1.1 Scenario 1: VR Controller Integration. In the first scenario, participants experienced six virtual materials selected based on the most frequently mentioned associations from our exploratory study (Section 4): rubber ($\mu \approx 0.9$), plastic ($\mu \approx 0.7$), leather ($\mu \approx 0.5$), wood ($\mu \approx 0.4$), glass ($\mu \approx 0.3$), and ice ($\mu \approx 0.2$). The Airveil device was mounted on a VR controller, and participants interacted by placing their index finger on the device surface while holding the controller (Figure 14 a).

We employed the 6×6 orifice plate with 0.1 mm openings for this implementation. This specific configuration was selected for its pneumatic versatility observed in Section 4: it uniquely supports a transition from bumpiness at low pressures (due to orifice turbulence) to a seamless, glass-like glide at high pressures, thereby effectively covering the wide textural dynamic range required for these diverse materials. Accordingly, each material was mapped to a specific air pressure level—0, 0.05, 0.11, 0.13, 0.15, and 0.17 bar, respectively—derived from the friction-pressure characterization curves (Section 4, Figure 7). This setup allowed participants to freely explore the virtual materials in VR and perceive the tactile differences directly through fingertip–surface interaction.

5.1.2 Scenario 2: Airveil-integrated 3D model scenario. In the second scenario, participants engaged in a customizable material-mapping task using two physical prototypes: a shoe and a humanoid figure.

For the shoe model, four distinct regions (top, side, body, bottom) were implemented, each featuring a different orifice plate configuration: 4×4 0.08 mm, 4×4 0.1 mm, 6×6 0.08 mm, and 6×6 0.1 mm. This diversity allowed participants to experience not only frictional differences but also variations in bumpiness driven by orifice density. Participants could assign materials from a set of six, with target friction coefficients set based on our exploratory study (Section 4): rubber ($\mu \approx 0.9$), plastic ($\mu \approx 0.7$), burlap ($\mu \approx 0.7$), leather ($\mu \approx 0.5$), wood ($\mu \approx 0.4$), and cotton ($\mu \approx 0.3$).

Crucially, to ensure consistent material friction rendering across the different hardware configurations, the air pressure required to achieve these target friction coefficients was individually calibrated for each orifice plate type. We referenced the specific friction-pressure mapping tables derived from our characterization study (Section 4, Figure 7) to determine the precise reference pressure values for each plate-material combination.

For the humanoid model, two regions (hat and clothes) were similarly customizable, implemented with 4×4 plates using 0.08 mm and 0.1 mm orifice sizes, respectively. In the VR environment, participants selected regions by touching them with their index finger, with active tactile areas limited to 1.5 × 1.5 cm. The corresponding physical 3D models were overlaid with liquid silicone rubber to ensure comfortable and consistent fingertip contact, and red circular markers were displayed in VR to indicate the designated touch regions. This scenario was specifically designed to validate that aerostatic friction modulation remains effective even when applied to the curved surfaces of physical props (Figure 14b).

5.1.3 Baseline Conditions: Vibration and Real Materials. To provide a rigorous comparative evaluation, participants evaluated the target materials in both scenarios under two additional baseline conditions:

(1) *Vibrotactile Feedback (Industry Standard):* we implemented friction approximations using the built-in linear resonant actuators (LRAs) of the Oculus Quest 3 controller. Drawing on modulation strategies established in prior psychophysical research [32], we adjusted the vibrotactile parameters to simulate different frictional states. Specifically, high-friction materials (*e.g.*, rubber, plastic) were simulated using lower-frequency, higher-amplitude pulses to mimic the mechanical "catch" of rough surfaces, whereas low-friction materials (*e.g.*, glass, ice) were approximated using continuous high-frequency, low-amplitude vibrations to convey smoothness. Participants held the standard controller (visualized as a virtual hand) and explored the same set of six materials. This comparison directly contrasts our *surface-property-change* mechanism against the industry-standard *kinetic-impulse* mechanism.

(2) *Physical Material Props:* To directly address the fidelity of our simulations, we provided participants with physical samples of all the target materials (Figure 14c). We meticulously selected these physical samples to ensure their static friction coefficients fell within an error margin of $\Delta\mu \leq 0.15$ compared to our system's target values. For Scenario 1 (VR Controller), participants explored these physical materials on a swatch board placed on a desk. For Scenario 2 (3D Models), to ensure geometric consistency, we fabricated duplicate replicas of the shoe and humanoid props and directly attached the physical material samples onto their corresponding target regions. This dual approach ensured that participants established a geometrically accurate perceptual anchor before evaluating the haptic interfaces.

To prevent learning and fatigue effects from skewing the results, the experimental order was strictly controlled. All participants completed the exact same total number of interactions across the two scenarios and the three feedback conditions (Airveil, Vibration, Physical Materials Props). The presentation order of the two scenarios, as well as the sequence of the three feedback methods within each scenario, were fully counterbalanced across participants. After completing all interactions, participants filled out questionnaires rating realism, distinguishability, enjoyment, and overall

preference, and provided open-ended comments. Throughout the experiment, participants wore noise-canceling headphones playing white noise to minimize auditory cues. The entire study procedure lasted approximately 30 minutes per participant.

5.1.4 Participants. Twelve participants (4 females, age: 22–35) took part in this study. All participants were right-handed, and their fingers were cleaned prior to touching the device to minimize residue effects. During the experiment, none of the participants reported any discomfort.

5.2 Quantitative Results

For our data analysis, given the non-parametric nature of the questionnaire ratings (ordinal Likert scales) and the strictly within-subjects design with three conditions (Airveil, Vibration, Physical Material Props), we utilized the Friedman test as the omnibus test to evaluate overall differences across the feedback methods. Where the Friedman test revealed a statistically significant main effect ($p < 0.05$), we conducted post-hoc pairwise comparisons using Wilcoxon signed-rank tests. To strictly control for Type I errors associated with multiple comparisons, a Bonferroni correction was applied, adjusting our significance threshold to $\alpha = 0.0167$ (0.053 comparisons).

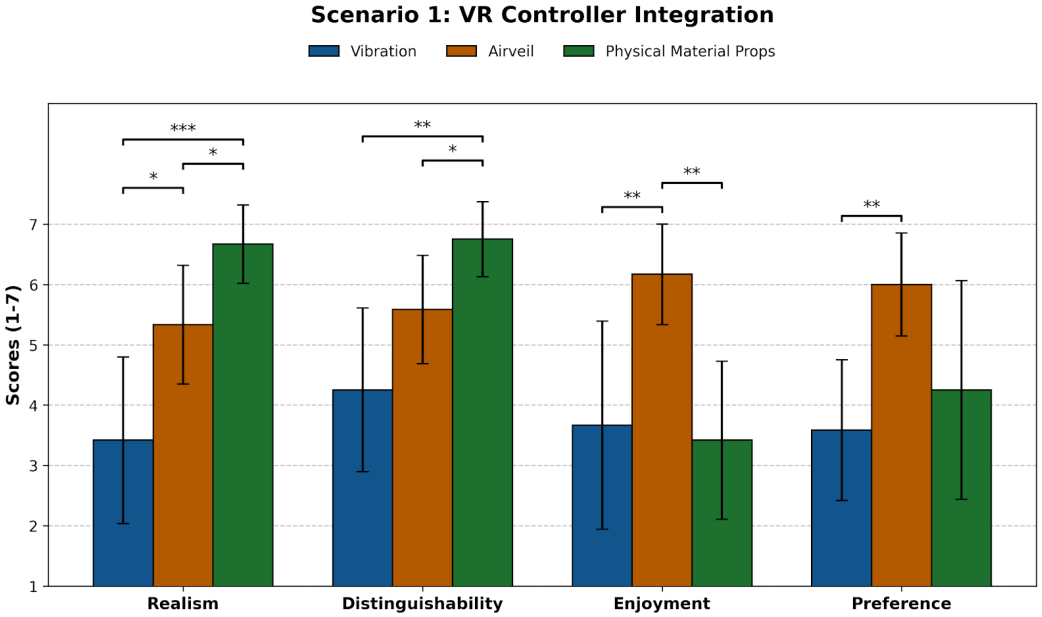

Fig. 15. Scenario 1 (VR Controller Integration): Comparison of mean user ratings across three feedback conditions (Vibration, Airveil, and Physical Material Props) evaluated on four dimensions: Realism, Distinguishability, Enjoyment, and Preference. Error bars represent standard deviations, and asterisks indicate statistical significance.

5.2.1 Scenario 1: VR Controller Integration. The results for the VR controller scenario are summarized in Figure 15. The Friedman test indicated significant differences among the three conditions across all four metrics: Realism, Distinguishability, Enjoyment, and Preference.

- Realism & Distinguishability: Post-hoc analysis revealed that Airveil was rated significantly higher than Vibration in both Realism ($p < 0.0167$) and Distinguishability ($p < 0.01$). While

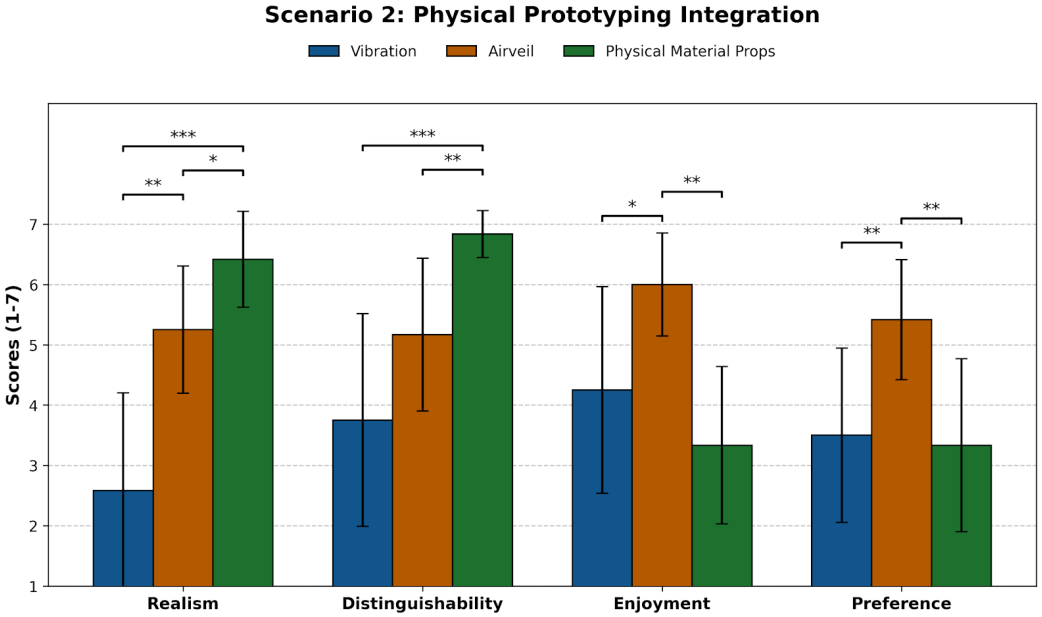

Fig. 16. Scenario 2 (Physical Prototyping Integration): Comparison of mean user ratings across three feedback conditions (Vibration, Airveil, and Physical Material Props) evaluated on four dimensions: Realism, Distinguishability, Enjoyment, and Preference. Error bars represent standard deviations, and asterisks indicate statistical significance.

Physical Material Props scored the highest, Airveil successfully bridged the gap, performing significantly better than the industry-standard vibration.

- Enjoyment & Preference: Airveil significantly outperformed both Vibration ($p < 0.01$) and Physical Material Props ($p < 0.01$) in terms of Enjoyment. For overall Preference, users significantly preferred Airveil over Vibration ($p < 0.01$). The high enjoyment ratings suggest that the air cushion modulation provided a uniquely engaging experience in VR compared to physical material props.

5.2.2 Scenario 2: Physical 3D Model Integration. The results for the 3D model scenario are summarized in Figure 16. Similar to Scenario 1, the omnibus Friedman test showed significant main effects across all metrics.

- Realism: Airveil yielded significantly higher Realism scores compared to Vibration ($p < 0.01$). Physical Material Props remained the upper bound ($p < 0.001$ vs. Vibration), but Airveil's performance closely approached this physical baseline.
- Distinguishability: Interestingly, when integrated into 3D models, Physical Material Props provided the highest distinguishability. Airveil and Vibration showed no significant difference from each other, though Airveil's mean score trended higher.
- Enjoyment & Preference: Airveil was clearly the favored method. It scored significantly higher in Enjoyment compared to Vibration ($p < 0.0167$) and Physical Material Props ($p < 0.01$). Likewise, for overall Preference, Airveil was rated significantly higher than both Vibration and Physical Material Props ($p < 0.01$).

Overall, the quantitative results robustly support our hypotheses. Airveil not only consistently outperforms conventional vibrotactile feedback in conveying realistic and distinguishable surface properties, but its dynamic friction modulation also makes it the most enjoyable and preferred haptic interaction method among users.

5.3 Qualitative Feedback

Beyond numerical ratings, participants' qualitative feedback provided deeper insights into the specific strengths of the aerostatic mechanism and the perceptual benefits across both application scenarios.

Material Fidelity and Realism. Consistent with the quantitative data, participants specifically praised Airveil's ability to render diverse surface properties, frequently comparing it favorably to the real physical references. For low-friction materials (*e.g.*, glass, ice), multiple participants (P1, P5, P9, P10) noted that the air-cushion feedback felt remarkably similar to touching the actual physical props. P10 emphasized that smooth surfaces were "much more convincingly rendered" with Airveil than with vibration, as it physically removed the dragging resistance rather than just masking it. Furthermore, participants observed that the high-friction renderings (*e.g.*, rubber, plastic) also closely mirrored the real physical materials, relying on the native friction of the silicone interface. Validating the advantage of true surface modulation, P5 explicitly stated, "Truly touching the surface makes the sensation feel much more realistic compared to just feeling a vibration," emphasizing how direct mechanoreceptor stimulation outperforms abstract oscillatory cues.

Immersion via Physical Integration. The study also validated the value of integrating Airveil into physical 3D props (Scenario 2). Participants (P2, P7, P8) reported that the direct interaction with the augmented object produced a profound sense of presence. Multiple participants emphasized that direct contact with the air cushion provided a "stronger sense of presence," noting that the combination of "seeing and touching the actual object" significantly enhanced the coherence between visual and haptic cues.

Limitations and Artifacts. While the feedback was predominantly positive, some minor artifacts were noted. A few participants mentioned the auditory noise produced when the finger directly occluded an air orifice, while others observed a slight cooling effect (thermal artifact) from the airflow on certain textures. These factors suggest avenues for future refinement in airflow management and acoustic dampening.

5.4 Summary

In summary, both the rigorous statistical analysis and user feedback robustly indicate that Airveil provides a significantly more realistic, distinguishable, and enjoyable tactile experience than traditional vibration-based feedback. By enabling true friction reduction that closely approximates the sensation of physical material props, and by supporting seamless integration into both ungrounded controllers and arbitrary 3D geometries, Airveil offers a versatile and high-fidelity solution for delivering tangible materiality in VR and mobile MR environments.

6 CONCLUSION

In this work, we presented Airveil, a novel haptic interface that leverages the air cushion effect (aerostatic lubrication) to dynamically modulate the tangential friction between the fingertip and a surface. Unlike conventional vibrotactile approaches that rely on creating tactile illusions via additive oscillation, Airveil introduces a subtractive friction modulation mechanism. By regulating the pressure distribution of an air film—governed by the Reynolds equation—our system physically reduces surface resistance to render a wide dynamic range of materiality, spanning from the high friction of rubber to the "super-smooth" glide of ice.

We detailed the design and fabrication of the micro-patterned interface and demonstrated its highly adaptable form factor by integrating it into both untethered VR controllers and arbitrary physical 3D props. Our rigorous psychophysical evaluations confirmed that Airveil's authentic physical modulation significantly outperforms illusory vibration-based feedback, closely approximating the tactile fidelity of actual physical material props in terms of realism, distinguishability, and enjoyment. By bridging the gap between visual fidelity and tactile reality in a highly versatile package, Airveil establishes a new paradigm for delivering immersive and tangible materiality across mobile, virtual, and mixed reality environments.

7 DISCUSSION AND FUTURE WORK

Our work introduces Airveil as a paradigm shift from traditional vibrotactile feedback to subtractive friction modulation. By validating the aerostatic lubrication mechanism, we have demonstrated a highly adaptable interface capable of rendering the "super-smooth" sensation of low-friction materials—a quality that has historically been elusive in ungrounded VR/MR haptics.

7.1 Expanding the Dynamic Range of Haptics

A key finding of this study is the capacity of Airveil to fundamentally expand the dynamic range of tactile rendering. While traditional vibrotactile actuators (e.g., LRAs) rely exclusively on additive oscillation to simulate roughness, they cannot physically alter the surface's inherent drag. Furthermore, existing friction modulation technologies (such as ultrasonic vibration or electroadhesion) are predominantly confined to rigid, flat 2D surfaces (e.g., glass touchscreens) and often operate by actively increasing resistance.

Airveil overcomes these morphological and functional limitations. By utilizing a flexible silicone interface, it enables true *subtractive* modulation on curved, arbitrary 3D geometries. It leverages the high baseline friction of silicone to natively simulate resistive materials like rubber or plastic, while actively injecting a high-pressure air film to reduce friction (down to $\mu \approx 0.2$) to simulate slippery surfaces like ice or glass. By accessing this previously unreachable "low-friction" portion of the tactile spectrum on a mobile form factor, Airveil unlocks a new dimension of material expression, enabling designers to craft nuanced experiences spanning from high-resistance traction to near-frictionless gliding.

7.2 Decoupling Texture from Friction

Our results from the exploratory study (Section 4) highlight the importance of *decoupling* geometric cues from physical resistance. We observed that while air pressure dominates the perception of adhesiveness (stickiness), the spatial layout of the orifice array governs the perception of bumpiness (texture grain). This suggests a layered design space for future haptic textures: designers can select a specific "base friction" (pressure level) to determine the material class (*e.g.*, metal vs. wood) and overlay a "spatial pattern" (orifice density) to define the surface finish (*e.g.*, polished vs. matte). This decoupling offers granular control over materiality that is fundamentally difficult to achieve with single-actuator vibrotactile systems.

7.3 Limitations and Future Directions

Thermal Artifacts as Multimodal Cues. Participants noted that prolonged use of the air cushion effect caused the contact surface to cool down due to convective heat transfer and air expansion. While currently a comfort limitation, this phenomenon presents an opportunity for *multimodal haptics*. Future iterations could integrate localized heating elements (*e.g.*, weak Peltier modules or resistive wire) to counteract this cooling. Alternatively, the cooling effect could be actively controlled to

render thermal material properties—simulating the cold touch of metal or glass versus the warmth of wood—thereby reinforcing the realism of the interaction.

Acoustic and Pneumatic Stability. As noted in our technical evaluation, high airflow can generate audible noise (hissing) and, at peak pressures (0.23 bar), pneumatic instability (flutter). While we mitigated noise with headphones in our study, future engineering work will focus on integrating silent piezoelectric pumps and optimizing nozzle geometry to ensure laminar flow. To address instability, advanced PID control algorithms could be implemented to dynamically smooth pressure fluctuations, ensuring stable feedback even at the limits of the device's operating range.

Miniaturization and Integration. Currently, Airveil relies on a tethered pneumatic source. A critical next step for fully realizing mobile MR applications is the miniaturization of the pneumatic delivery system. Integrating wearable micro-compressors or onboard pressurized cartridges (*e.g.*, CO_2 canisters) will eliminate the tether, fully unleashing Airveil's potential for untethered, mobile haptic interactions. Beyond handheld mobility, its lightweight end-effector design also creates opportunities for integration with actuated mechanical structures. We envision mounting Airveil on robotic arms or force-feedback exoskeletons to combine fine surface rendering with kinesthetic force feedback, supporting both mobile devices and tangible interactions in shared spatial environments.

7.4 Closing Remarks

In summary, our findings validate the potential of air cushion based haptics as a powerful medium for enhancing virtual and physical interactions. By bridging the gap between visual expectations and tactile reality through aerostatic lubrication, Airveil paves the way toward more immersive, adaptable, and physically grounded experiences in the next generation of mobile MR and VR interfaces.

ACKNOWLEDGMENTS

This work was partly supported by the National Science and Technology Council (NSTC), Taiwan (under NTSC 114-2221-E-002-218-MY3, 114-2218-E-002-006, 114-2628-E-004 -001 -MY4, and 114-2221-E-004 -005), National Taiwan University (114L900902 and 115L8909) funded through the Ministry of Education (MOE), Taiwan, and National Chengchi University.

REFERENCES

[1] Michel Amberg, Frédéric Giraud, Betty Semail, Paolo Olivo, Géry Casiez, and Nicolas Roussel. 2011. STIMTAC: a tactile input device with programmable friction. In *Proceedings of the 24th annual ACM symposium adjunct on User interface software and technology*. 7–8.

[2] Shuhei Asano, Shogo Okamoto, and Yoji Yamada. 2014. Vibrotactile stimulation to increase and decrease texture roughness. *IEEE Transactions on Human-Machine Systems* 45, 3 (2014), 393–398.

[3] Cagatay Basdogan, Frederic Giraud, Vincent Levesque, and Seungmoon Choi. 2020. A review of surface haptics: Enabling tactile effects on touch surfaces. *IEEE transactions on haptics* 13, 3 (2020), 450–470.

[4] Olivier Bau and Ivan Poupyrev. 2012. REVEL: tactile feedback technology for augmented reality. *ACM Transactions on Graphics (TOG)* 31, 4 (2012), 1–11.

[5] Olivier Bau, Ivan Poupyrev, Ali Israr, and Chris Harrison. 2010. TeslaTouch: electrovibration for touch surfaces. In *Proceedings of the 23nd annual ACM symposium on User interface software and technology*. 283–292.

[6] Hrvoje Benko, Christian Holz, Mike Sinclair, and Eyal Ofek. 2016. Normaltouch and texturetouch: High-fidelity 3d haptic shape rendering on handheld virtual reality controllers. In *Proceedings of the 29th annual symposium on user interface software and technology*. 717–728.

[7] Sliman J Bensmaïa and Mark Hollins. 2003. The vibrations of texture. *Somatosensory & motor research* 20, 1 (2003), 33–43.

[8] Mélisande Biet, Frédéric Giraud, and Betty Lemaire-Semail. 2008. Squeeze film effect for the design of an ultrasonic tactile plate. *IEEE transactions on ultrasonics, ferroelectrics, and frequency control* 54, 12 (2008), 2678–2688.

[9] Shaoyu Cai, Zhenlin Chen, Haichen Gao, Ya Huang, Qi Zhang, Xinge Yu, and Kening Zhu. 2024. Vibopneumo: A vibratory-pneumatic finger-worn haptic device for altering perceived texture roughness in mixed reality. *IEEE Transactions on Visualization and Computer Graphics* (2024).

[10] Tom Carter, Sue Ann Seah, Benjamin Long, Bruce Drinkwater, and Sriram Subramanian. 2013. UltraHaptics: multi-point mid-air haptic feedback for touch surfaces. In *Proceedings of the 26th annual ACM symposium on User interface software and technology*. 505–514.

[11] Erik C Chubb, J Edward Colgate, and Michael A Peshkin. 2010. Shiverpad: A glass haptic surface that produces shear force on a bare finger. *IEEE Transactions on Haptics* 3, 3 (2010), 189–198.

[12] Heather Culbertson and Katherine J Kuchenbecker. 2017. Ungrounded haptic augmented reality system for displaying roughness and friction. *IEEE/ASME Transactions on Mechatronics* 22, 4 (2017), 1839–1849.

[13] Siegfried Derler and L-C Gerhardt. 2012. Tribology of skin: review and analysis of experimental results for the friction coefficient of human skin. *Tribology Letters* 45, 1 (2012), 1–27.

[14] Ramona Fagiani and Marco Barbieri. 2016. A contact mechanics interpretation of the duplex theory of tactile texture perception. *Tribology International* 101 (2016), 49–58.

[15] Sebastjan Glinsek, Mohamed Aymen Mahjoub, Matthieu Rupin, Tony Schenk, Nicolas Godard, Stéphanie Girod, Jean-Baptiste Chemin, Renaud Leturcq, Nathalie Valle, Sébastien Klein, et al. 2020. Fully transparent friction-modulation haptic device based on piezoelectric thin film. *Advanced Functional Materials* 30, 36 (2020), 2003539.

[16] Mohammad Shadman Hashem, Joolekha Bibi Joolee, Waseem Hassan, and Seokhee Jeon. 2021. Soft pneumatic fingertip actuator incorporating a dual air chamber to generate multi-mode simultaneous tactile feedback. *Applied Sciences* 12, 1 (2021), 175.

[17] Mohammad Shadman Hashem, Joolekha Bibi Joolee, Waseem Hassan, and Seokhee Jeon. 2023. Multi-mode Simultaneous Tactile Feedback Using Soft Pneumatic Fingertip Actuator with Dual Air Chamber. In *International Conference on Intelligent Autonomous Systems*. Springer, 617–620.

[18] Hwan Kim, HyeonBeom Yi, Hyein Lee, and Woohun Lee. 2018. HapCube: A wearable tactile device to provide tangential and normal pseudo-force feedback on a fingertip. In *Proceedings of the 2018 CHI Conference on Human Factors in Computing Systems*. 1–13.

[19] Guillaume J Laurent, Anne Delettre, and Nadine Le Fort-Piat. 2011. A new aerodynamic-traction principle for handling products on an air cushion. *IEEE Transactions on robotics* 27, 2 (2011), 379–384.

[20] Chi-Jung Lee, Hsin-Ruey Tsai, and Bing-Yu Chen. 2021. Hairtouch: Providing stiffness, roughness and surface height differences using reconfigurable brush hairs on a vr controller. In *Proceedings of the 2021 CHI Conference on Human Factors in Computing Systems*. 1–13.

[21] Vincent Levesque and Vincent Hayward. 2003. Experimental evidence of lateral skin strain during tactile exploration. In *Proceedings of EUROHAPTICS*, Vol. 2003. IEEE Dublin, 6–9.

[22] Jo-Yu Lo, Da-Yuan Huang, Chen-Kuo Sun, Chu-En Hou, and Bing-Yu Chen. 2018. RollingStone: Using single slip taxel for enhancing active finger exploration with a virtual reality controller. In *Proceedings of the 31st Annual ACM Symposium on User Interface Software and Technology*. 839–851.

[23] Alex Mazursky, Jacob Serfaty, and Pedro Lopes. 2024. Stick&Slip: Altering Fingerpad Friction via Liquid Coatings. In *Proceedings of the 2024 CHI Conference on Human Factors in Computing Systems*. 1–14.

[24] David J Meyer, Michael A Peshkin, and J Edward Colgate. 2013. Fingertip friction modulation due to electrostatic attraction. In *2013 world haptics conference (WHC)*. IEEE, 43–48.

[25] Abhijeet Mishra, Piyush Kumar, Jainendra Shukla, and Aman Parnami. 2022. HaptiDrag: A device with the ability to generate varying levels of drag (friction) effects on real surfaces. *Proceedings of the ACM on Interactive, Mobile, Wearable and Ubiquitous Technologies* 6, 3 (2022), 1–26.

[26] Shogo Okamoto, Hikaru Nagano, and Yoji Yamada. 2012. Psychophysical dimensions of tactile perception of textures. *IEEE Transactions on Haptics* 6, 1 (2012), 81–93.

[27] Osborne Reynolds. 1886. On the theory of lubrication and its application to Mr. Beauchamp Tower's experiments, including an experimental determination of the viscosity of olive oil. *Philosophical transactions of the Royal Society of London* 177 (1886), 157–234.

[28] Steeven Villa Salazar, Claudio Pacchierotti, Xavier De Tinguy, Anderson Maciel, and Maud Marchal. 2020. Altering the stiffness, friction, and shape perception of tangible objects in virtual reality using wearable haptics. *IEEE transactions on haptics* 13, 1 (2020), 167–174.

[29] Thomas Sednaoui, Eric Vezzoli, Brygida Dzidek, Betty Lemaire-Semail, Cedrick Chappaz, and Michael Adams. 2017. Friction reduction through ultrasonic vibration part 2: Experimental evaluation of intermittent contact and squeeze film levitation. *IEEE Transactions on Haptics* 10, 2 (2017), 208–216.

[30] Craig D Shultz, Michael A Peshkin, and J Edward Colgate. 2018. On the electrical characterization of electroadhesive displays and the prominent interfacial gap impedance associated with sliding fingertips. In *2018 IEEE Haptics Symposium (HAPTICS)*. IEEE, 151–157.

[31] Rajinder Sodhi, Ivan Poupyrev, Matthew Glisson, and Ali Israr. 2013. AIREAL: interactive tactile experiences in free air. *ACM Transactions on Graphics (TOG)* 32, 4 (2013), 1–10.

[32] Paul Strohmeier and Kasper Hornbæk. 2017. Generating haptic textures with a vibrotactile actuator. In *Proceedings of the 2017 CHI Conference on Human Factors in Computing Systems*. 4994–5005.

[33] M Takasaki, D Yamaguchi, Y Ochiai, T Hoshi, and T Mizuno. 2015. Between smoothness and stickiness. In *2015 IEEE World Haptics Conference [D-46]*.

[34] Sarah Elizabeth Tomlinson. 2009. *Understanding the friction between human fingers and contacting surfaces*. Ph. D. Dissertation. University of Sheffield.

[35] Chih-An Tsao, Tzu-Chun Wu, Hsin-Ruey Tsai, Tzu-Yun Wei, Fang-Ying Liao, Sean Chapman, and Bing-Yu Chen. 2022. Frictshoes: Providing multilevel nonuniform friction feedback on shoes in vr. *IEEE Transactions on Visualization and Computer Graphics* 28, 5 (2022), 2026–2036.

[36] Eric Vezzoli, Zlatko Vidrih, Vincenzo Giamundo, Betty Lemaire-Semail, Frédéric Giraud, Tomaz Rodic, Djordje Peric, and Michael Adams. 2017. Friction reduction through ultrasonic vibration part 1: Modelling intermittent contact. *IEEE transactions on haptics* 10, 2 (2017), 196–207.

[37] Toshio Watanabe and Shigehisa Fukui. 1995. A method for controlling tactile sensation of surface roughness using ultrasonic vibration. In *Proceedings of 1995 IEEE International Conference on Robotics and Automation*, Vol. 1. IEEE, 1134–1139.

[38] Eric Whitmire, Hrvoje Benko, Christian Holz, Eyal Ofek, and Mike Sinclair. 2018. Haptic revolver: Touch, shear, texture, and shape rendering on a reconfigurable virtual reality controller. In *Proceedings of the 2018 CHI conference on human factors in computing systems*. 1–12.

[39] Michaël Wiertlewski, Rebecca Fenton Friesen, and J Edward Colgate. 2016. Partial squeeze film levitation modulates fingertip friction. *Proceedings of the national academy of sciences* 113, 33 (2016), 9210–9215.

[40] Laura Winfield, John Glassmire, J Edward Colgate, and Michael Peshkin. 2007. T-pad: Tactile pattern display through variable friction reduction. In *Second Joint EuroHaptics Conference and Symposium on Haptic Interfaces for Virtual Environment and Teleoperator Systems (WHC'07)*. IEEE, 421–426.

[41] Wei Zhong, Zhiyuan Ge, Xin Li, Guoliang Tao, and Toshiharu Kagawa. 2015. Basic investigation of a contactless air conveyor for flat products using viscous traction. In *2015 International Conference on Fluid Power and Mechatronics (FPM)*. IEEE, 374–378.

[42] Li Zhu, Didier El-Baz, and Huangsheng Ning. 2015. Survey on air levitation conveyors with possible scalability properties. In *2015 IEEE 12th Intl Conf on Ubiquitous Intelligence and Computing and 2015 IEEE 12th Intl Conf on Autonomic and Trusted Computing and 2015 IEEE 15th Intl Conf on Scalable Computing and Communications and Its Associated Workshops (UIC-ATC-ScalCom)*. IEEE, 802–807.